Optimization of sensitivity in Long Period Fiber Gratings with overlay deposition

Ignacio Del Villar, Ignacio R. Matías and Francisco J. Arregui

Departamento de Ingeniería Eléctrica y Electrónica, Universidad Pública de Navarra, 31006 Pamplona, Spain.
ignacio.delvillar@unavarra.es, natxo@unavarra.es , parregui@unavarra.es

Philippe Lalanne

Institut d'Optique Centre National de la Recherche Scientifique BP 147 Orsay 91 403 France.
philippe.lalanne@iota.u-psud.fr.

Abstract: The deposition of an overlay of higher refractive index than the cladding in a Long Period Fiber Grating (LPFG) permits to improve the sensitivity to ambient refractive index changes in a great manner. When the overlay is thick enough, one of the cladding modes is guided by the overlay. This causes important shifts in the effective index values of the cladding modes, and henceforward fast shifts of the resonance wavelength of the attenuations bands in the transmission spectrum. This could be applied for improving the sensitivity of LPFG sensors. The problem is analysed with a numerical method based on LP mode approximation and coupled mode theory, which agrees with so far published experimental results.

OCIS codes: (050.2770) Gratings, (060.2430) Fibers, single-mode, (260.2110) Electromagnetic theory, (310.1860) Deposition and fabrication.

References and links

1. J. R.Qiang and H. E. Chen, "Gain flattening fibre filters using phase shifted long period fibre grating," Electron. Lett. **34**, 1132-1133 (1998).
2. A. M. Vengsarkar, P. J. Lemaire, J. B. Judkins, V. Bhatia, T. Erdogan, and J. E. Sipe, "Long-period fiber gratings as Band Rejection Filters," J. Lightwave Technol. **14**, 58-65 (1996).
3. B. J. Eggleton, R. E. Slusher, J. B. Judkins, J. B. Stark and A. M. Vengsarkar, "All-optical switching in long period fiber gratings," Opt. Lett. **22**, 883-885 (1997).
4. K. W. Chung, S. Yin, "Analysis of widely tunable long-period grating by use of an ultrathin cladding layer and higher-order cladding mode coupling," Opt. Lett. **29**, 812-814 (2004).
5. V. Bhatia and A. M. Vengsarkar, "Optical fiber long-period grating sensors," Opt. Lett. **21**, 692-694 (1996).
6. V. Bhatia, "Applications of long-period gratings to single and multi-parameter sensing," Opt. Exp. **4**, 457-466 (1999), http://www.opticsexpress.org/abstract.cfm?URI=OPEX-4-11-457.
7. Y. G. Han, S. B. Lee, C. S. Kim, J. U. Kang, U. C. Paek and Y. Chung, "Simultaneous measurement of temperature and strain using dual long-period fiber gratings with controlled temperature and strain sensitivities," Opt. Exp. **11**, 476-481 (2003), http://www.opticsexpress.org/abstract.cfm?URI=OPEX-11-5-476.
8. C. C. Ye, S. W. James and R. P. Tatam, "Simultaneous temperature and bend sensing using using long-period fiber gratings," Opt. Lett. **25**, 1007-1009 (2000).
9. H. J. Patrick, A. D. Kersey and F. Bucholtz, "Analysis of the response of long period fiber gratings to external index of refraction," J. Lightwave Technol. **16**, 1606-1612 (1998).
10. R. Hou, Z. Ghassemlooy, A. Hassan, C. Lu and K. P. Dowker, "Modelling of long-period fibre grating response to refractive index higher than that of cladding," Meas. Sci. Technol. **12**, 1709-1713 (2001).
11. S. T. Lee, R. D. Kumar, P. S. Kumar, P. Radhakrishnan, C. P. G. Vallabhan, V. P. N. Nampoori, "Long period gratings in multimode optical fibers: application in chemical sensing," Opt. Comm. **224**, 237-241 (2003).
12. N. D. Rees, S. W. James, R. P. Tatam and G. J. Ashwell, "Optical fiber long-period gratings with Langmuir-Blodgett thin-film overlays," Opt. Lett. **27**, 686-688 (2002).
13. S. W. James and R. P. Tatam, "Optical fibre long-period grating sensors: characteristics and application," Meas. Sci Technol. **14**, R49-R61 (2003).

#5675 - $15.00 US Received 8 November 2004; revised 20 December 2004; accepted 20 December 2004

14. E. Anemogiannis, E. N. Glytsis and T. K. Gaylord, "Transmission characteristics of long- period fiber gratings having arbitrary azimutal/radial refractive index variation," J. Lightwave Technol. **21**, 218-227 (2003).
15. T. Erdogan, "Fiber Grating Spectra," J. Lightwave Technol. **15**, 1277-1294 (1997).
16. T. Erdogan, "Cladding-mode resonances in short- and long-period fiber gratings filters," J. Opt. Soc. Am. A, **14**, 1760-1773 (1997).
17. D. B. Stegall and T. Erdogan, "Leaky cladding mode propagation in long-period fiber grating devices," IEEE Photon. Technol. Lett. **11**, 343-345 (1999).
18. Y. Koyamada, "Numerical analysis of core-mode to radiation-mode coupling in long-period fiber gratings," IEEE Photon. Technol. Lett. **13**, 308-310 (2001).
19. I. Del Villar, M. Achaerandio, I. R. Matías and F. J. Arregui, "Deposition of an Overlay with Electrostactic Self-Assembly Method in Long Period Fiber Gratings," Opt. Lett. In press.
20. K. Morishita, "Numerical analysis of pulse broadening in grated index optical fibers," IEEE Trans. Microwave Theory Tech. **29**, 348-352 (1981).
21. D. Gloge, "Weakly guiding fibers," App. Opt. **10**, 2252-2258 (1971).
22. A. K. Ghatak, K. Thyagarajan, and M. R. Shenoy, IEEE J. Lightwave Technol. **5,** 660- 667(1987).
23. A. W. Snyder and J. D. Love, *Optical waveguide theory* (London U.K: Chapman and Hall, 1983).
24. K. Skjonnemand, "Optical and structural characterisation of ultra thin films," Ph.D. disseration (Cranfield University, Bedford, UK, 2000).
25. G. Decher, "Fuzzy nanoassemblies: toward layered polymeric multicomposites," Science, **277**, 1232-1237 (1997).
26. S. A. Khodier, "Refractive index of standard oils as a function of wavelength and temperature," Optics & Laser Tech., **34**, 125-128 (2002).

1. Introduction

Long Period Fiber Gratings (LPFGs) consist of a periodic index modulation of the refractive index of the core of a single mode fiber (SMF), with a much longer period than Fiber Bragg Gratings (FBGs). They have found many applications during the nineties in optical communications and sensors fields. In optical communications many devices have been developed, such as gain equalizers [1], band rejection filters [2], tunable filters [3] and optical switches [4]. In sensors field, if compared with FBGs, they are also sensitive to measurands such as strain or temperature [5-8], which may alter the period of the grating or the refractive of the core or cladding. Nonetheless, modes couple in a different way with respect to FBGs, which improves the characteristics of sensors in a great manner. LPFGs are highly sensitive to the surrounding media, which also includes the drawback of a dependence on temperature. Anyway, there exist techniques for avoiding this problem [7, 8], which permits at the same time multi-parameter sensing [6]. They also present low background reflections and insertion losses, and demodulation schemes are economical. All these good properties make LPFGs adequate for more purposes than strain or temperature detection. They can be used as refractometers [9, 10], or for detection of chemical substances in the ambient [11]. Furthermore, if an overlay is deposited on the cladding, its refractive index will modify the coupling of modes [12]. If the material selected is sensitive to a specific parameter, highly sensitive and specific devices will be obtained.

Regarding the fabrication, LPFGs can be obtained with several techniques, being ultraviolet (UV) irradiation the most extended one. Others are ion implantation, irradiation by femtosecond pulses in the infrared, irradiation by CO_2 lasers, diffusion of dopants into the core, relaxation of mechanical stress, and electrical discharges. A good review on these techniques can be found in [13].

Typically, the periodicity of LPFGs ranges between 100μm to 1mm. As a result, dips are created in the transmission spectrum at wavelengths where there is a coupling between the core and copropagating cladding modes, unlike in FBGs, where there is a coupling between contrapropagating modes. Each attenuation band presents a minimum, notated as resonance wavelength. This wavelength value is in close relation with the one that satisfies the Bragg condition between the coupled modes. A much better approximation can be obtained if the influence of the self coupling coefficient of the modes is included in the formulation [14], as it

#5675 - $15.00 US Received 8 November 2004; revised 20 December 2004; accepted 20 December 2004

will be explained in next section. The third possibility is to solve the coupled mode equations. The consideration of all coupling coefficients will permit to obtain more exact values for the resonance wavelengths and the transmission spectrum. The drawback of this option is a higher computational effort in comparison with the other two, where no differential equation has to be solved.

Regarding the depth of the attenuation bands, there are many factors that influence this value. The two most important ones are the cross coupling coefficient between the core mode and the cladding mode that couples at that resonance wavelength, and the length of the grating. A simple formula permits to have an approximate idea of the exact value [13, 15]:

$$T_i = 1 - \sin^2(k_i L) \tag{1}$$

where k_i is the coupling coefficient of the *i*th cladding mode, L the length of the grating and T_i minimum transmission of the attenuation band created by coupling between the core mode and the *i*th cladding mode.

Henceforward, the modulation of the grating is critical, because the coupling coefficients are directly proportional to this value. Consequently, LPFGs can be classified into weak and strong LPFGs [16].

Regarding the analysis of LPFGs, two different cases have been studied so far. Until now we have considered for the explanations the first one, where it is assumed that the ambient refractive index is lower than cladding [16]. As the ambient refractive index approaches that of the cladding, the sensitivity of the resonance wavelength to variations of the ambient refractive index is higher. Then, the second case starts when the ambient refractive index exceeds that of the cladding. The core couples with radiation modes [10,17,18] and the dependence of the resonance wavelength on the ambient refractive index is not so accused. Instead, the resonance depth is more dependent on this parameter for values close to the refractive index of the cladding [9]. In both cases, the region of highest sensitivity is located around the refractive index of the cladding.

In this work, a third possibility is presented. In the previous two cases, the cladding was surrounded by a medium of infinite thickness. Now a thin overlay of higher refractive index than the cladding is deposited between the cladding and the infinite thickness surrounding media. One of the cladding modes will be guided by the overlay if it is thick enough. This causes a reorganization of the effective indices of the modes of the cladding. As a result, there are important variations of the Bragg condition, which leads to dramatic shifts of the resonance wavelengths if we work around the thickness value where there is a transition to guidance of a mode in the overlay. The aim will be to select an adequate refractive index and thickness of the overlay, in order to increase the sensitivity of the effective index of the cladding modes for a specific application.

The shift is maximum when the effective index of the mode is half way between its original effective index and the original effective index before deposition of the next lower cladding mode. Consequently, there is an optimum overlay thickness (OOT). The value of the OOT depends mainly on the refractive index of the material deposited and on the ambient. In first place, the refractive index of the overlay is fixed. This fact defines the amount of material that is necessary to deposit and the sensitivity of the refractometer. Secondly, an optimum thickness value is calculated for the middle value of the ambient refractive index range where the refractometer will operate. In this way, highly sensitive refractometers can be designed for small refractive index ranges. On the other hand, if the OOT is calculated for a material whose refractive index varies with some parameter, the sensitivity of LPFG can be improved in many sensor fields: chemical sensors, biosensors, inmunoassays and so on.

So far, Electrostatic Self-Assembly (ESA) [19] and Langmuir Blodgett (LB) [12] techniques have been applied for the deposition of an overlay of tens of nanometers. In this work it is assumed that the refractive index of the material deposited is purely real, which is not the case in the case in ESA and LB techniques. However, this assumption permits to understand more easily the effects of deposition of an overlay on an LPFG, and it still predicts

#5675 - $15.00 US Received 8 November 2004; revised 20 December 2004; accepted 20 December 2004

adequately experimental results in [12] and [19]. In a future work it will be analysed the deposition of an overlay with losses, which is more complex.

The numerical method used for determining the wavelength that satisfies the Bragg condition between the core mode and each cladding mode, and the transmittance of the LPG is based on that described in [14]. Coupled mode theory is the basis for the calculation of LP modes in a cylindrical multilayer waveguide and it is explained in next section. In section 3 the explanation of the effects of a thin overlay on an LPFG and its applications are presented. Finally, some conclusions are given in section 4.

2. Theory

So far coupled mode theory has proved to be a powerful tool for simulation of LPFG structures. In [16] a three layer model is presented, where the transmission can be accurately obtained provided the ambient refractive index is lower than the cladding. If the ambient refractive index is higher than the cladding, other approximations are necessary [10, 17, 18]. The method used in this chapter is based on that presented in [14] and it includes three steps.

2.1 Calculation of the propagation constants of LP modes

The problem analysed in this work (see Fig. 1) presents four layers. The calculation of the modes in a cylindrical multilayer waveguide becomes a difficult and computational expensive task.

To avoid this problem, in [14, 20] a theoretical model is described. It is based on scalar approximation analysis to obtain the LP modes of a cylindrical dielectric waveguide. LP modes are adequate for description of a cylindrical waveguide under assumption of weak guidance [21]. But in [14] it is proved that the high contrast between ambient and cladding refractive indices plays no important role in the results. Consequently, the presence of an overlay of a refractive index which shows not important contrast with the cladding will not affect to the results in a great manner, provided low LP modes are analysed. As the material deposited on the cladding shows a higher contrast, error present in the results will increase, but results will remain qualitatively correct. LPνj modes (ν=0) are everywhere polarized in the same direction, or in other words the fields are plane polarized. Nonetheless, the fields of higher order LPνj modes are not plane polarized and it is proved in [14] that they play a role in the results obtained in LPFGs. The reason is that the irradiation for the generation of the grating is not symmetric around the fiber. However, for the sake of simplicity, it will be assumed that the structure simulated presents no azimutal variation of the perturbed index profile after exposure to UV radiation. In this way, there are only interactions between LP0j modes, and each mode is not treated as two independent modes, as it is the case for ν>0 modes.

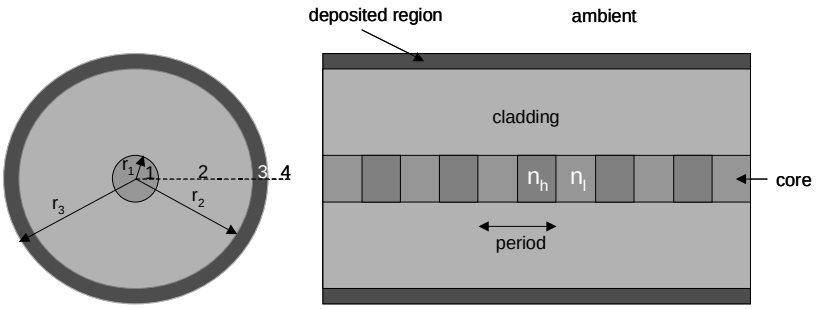

Fig. 1. Transversal and longitudinal section of LPFG structure deposition of an overlay on the cladding.

After solving the following scalar equation [22]:

#5675 - $15.00 US Received 8 November 2004; revised 20 December 2004; accepted 20 December 2004

$$\frac{d^2u}{dr^2}+\left[k_0^2\tilde{n}^2(r)-\beta^2\right]u=0 \tag{2}$$

where k0 = 2π/λ, λ is the freespace wavelength, β is the propagation constant of a mode, r is the radius, $\tilde{n}$ is defined by:

$$\tilde{n}^2=n^2(r)-\frac{\nu^2-\frac{1}{4}}{k_0^2r^2} \qquad \nu=0 \tag{3}$$

where n is the refractive index as a function of the radius and ν is the azimutal order, and u is defined by:

$$u(r)=\frac{R(r)}{\sqrt{r}} \tag{4}$$

where R(r) is the radial variation of the modal field.

The transverse electric field component propagating along the z-axis is given by:

$$U_{0j,i}(r,\phi,z)=\exp(-j\beta_{0j}z)\Psi_{0j,i}(r,\phi)=\exp(-j\beta_{0j}z)\Phi(\phi)R_{0j,i}(r)=$$
$$=\exp(-j\beta_{0j}z)\times\begin{cases}A_{0j,i}J_0(r\gamma_{0j,i})+B_{0j,i}Y_0(r\gamma_{0j,i})\\ A_{0j,i}I_0(r\gamma_{0j,i})+B_{0j,i}K_0(r\gamma_{0j,i})\end{cases}\text{ when }\begin{matrix}\beta_{0j}<k_0n_i\\ \beta_{0j}>k_0n_i\end{matrix} \tag{5}$$

where β_{0j} is the propagation constant of the LP_{0j} mode, $\gamma_{0j,i}=\sqrt{\left|k_0^2n_i^2-\beta_{0j}^2\right|}$ is the magnitude of the transverse wavenumber, ϕ is the azimutal angle, and $A_{0j,i}$ and $B_{0j,i}$ are not normalized field expansion coefficients determined by the boundary conditions within the cylindrical layer i. $J_0(r\gamma_{0j,i})$ and $Y_0(r\gamma_{0j,i})$ are the ordinary Bessel functions of first and second kind of order 0, while $I_0(r\gamma_{0j,i})$ and $K_0(r\gamma_{0j,i})$ are the modified Bessel functions of first and second kind of order 0.

After this, the Transfer Matrix Method (TMM) [14,20] is applied for the calculation of the propagation constants of the four layer cylindrical waveguide problem. At the same time the coefficients $A_{0j,i}$ and $B_{0j,i}$ in each layer will be calculated and normalized so that each mode carries the same power P0:

$$P_{0j}=\frac{\beta_{0j}}{2\omega\mu_0}\int_{\phi=0}^{2\pi}d\phi\int_{r=0}^{r_1}R_{0j}(r)R_{0j}(r)rdr \tag{6}$$

2.2. Derivation of coupling coefficients

According to coupled mode theory [14, 16, 23], the interaction between optical modes is proportional to their coupling coefficient. The contribution of longitudinal coupling coefficient in coupled mode analysis can be neglected [14, 15, 16]. Consequently we will refer to the transversal coupling coefficient as the general coupling coefficient. In cylindrical coordinates the coupling coefficient between each two modes can be expressed as:

$$K_{vj,\mu k}=\frac{\omega}{4P_0}\times\int_{\phi=0}^{2\pi}\int_{r=0}^{\infty}\Delta\varepsilon(r,\phi,z)\Psi_{vj}(r,\phi)\Psi_{\mu k}(r,\phi)rdrd\phi \tag{7}$$

where Ψ(r,ϕ) is the transverse field for an LP mode as expressed in Eq. (5) and Δε(r,ϕ,z) is the permittivity variation. There is no azimutal variation of the perturbed index profile, and there is weak guidance between the core and the cladding of the fiber. Consequently, the permittivity can be expressed as:

#5675 - $15.00 US Received 8 November 2004; revised 20 December 2004; accepted 20 December 2004

$$\Delta\varepsilon(r,z) \approx 2\varepsilon_0 n_0(r)\Delta n(r,z) \tag{8}$$

where ε_0 is the freespace permittivity, $n_0(r)$ is the refractive index profile of the structure without the perturbation, and $\Delta n(r,z)$ is the variation of the refractive index. This last variable is the product of a perturbation constant and two other functions:

$$\Delta n(r,z) = p(r)\sigma(z)S(z) \tag{9}$$

where p(r) is the transverse refractive index perturbation. $\sigma(z)$ is the apodization factor, and S(z) is the longitudinal refractive index perturbation factor. It will be approximated by a Fourier series of two terms:

$$S(z) = s_0 + s_1 \cos\left((2\pi/\Lambda)z\right) \tag{10}$$

where Λ is the period of the grating.

After these approximations, the coupling coefficients will be expressed as:

$$K_{vj,\mu k} = \left[s_0 + s_1 \cos\left(\left(\frac{2\pi}{\Lambda}\right)z\right)\right]\frac{\omega\varepsilon_0}{2P_0}\times\int_{\phi=0}^{2\pi}\int_{r=0}^{\infty} n_0(r)p(r)\Psi_{vj}(r,\phi)\Psi_{\mu k}(r,\phi)rdrd\phi =$$

$$= \left[s_0 + s_1 \cos\left(\left(\frac{2\pi}{\Lambda}\right)z\right)\right]\varsigma_{vj,\mu k} \tag{11}$$

where $\varsigma_{vj,\mu k}$ is the coupling constant, even though it can show a slow 'z' varying dependence [16]. From now on, this value will be considered the coupling coefficient and $K_{vj,\mu k}$ will not be used in the formulation for coupled mode differential equations.

Under the assumption of a uniform index perturbation within the core of the fiber, the interactions occur between LP_{0k} modes. As a result, there is no azimutal dependence and expression (8) of [14] can be simplified for the coupling coefficient:

$$\varsigma_{0j,0k} = \frac{\omega\varepsilon_0}{2P_0} n_0(r_1)p(r_1)\int_{\phi=0}^{2\pi} d\phi\int_{r=0}^{r_1} R_{0j}(r)R_{0k}(r)rdr \tag{12}$$

Otherwise, the LP modes of higher azimutal order should be treated as two independent modes. An important reduction in computation time can be obtained if only half of the coupling coefficients are calculated. This can be obtained if the symmetry property is used: $\varsigma_{0j,0k} = \varsigma_{0k,0j}$.

2.3. Coupled mode equations

After deduction of the propagation constants of the modes and the coupling coefficients, coupled mode theory will be introduced. Unlike in FBGs, backward propagating modes will be neglected. In this way, the generalized coupled mode equations describing an LPG can be expressed as [14, 16]:

$$\frac{dF_{0k}(z)}{dz} = -j\sum_{j=1}^{M} K_{0j,0k}F_{0j}(z)\exp\left(-j\left(\beta_{0j}-\beta_{0k}\right)z\right) \quad \text{for } k=1,2,\ldots M. \tag{13}$$

This can be expressed in a matrix form in the following way:

$$\begin{pmatrix} \dot{F}_{01}(z) \\ \dot{F}_{02}(z) \\ \vdots \\ \dot{F}_{0N}(z) \end{pmatrix} = \begin{pmatrix} Q_{01} & V_{02,01} & \cdots & V_{0N,01} \\ V_{01,02} & Q_{02} & \cdots & V_{0N,02} \\ \vdots & \vdots & \ddots & \vdots \\ V_{01,0N} & V_{02,0N} & \cdots & Q_{0N} \end{pmatrix} \begin{pmatrix} F_{01}(z) \\ F_{02}(z) \\ \vdots \\ F_{0N}(z) \end{pmatrix} \tag{14}$$

#5675 - $15.00 US Received 8 November 2004; revised 20 December 2004; accepted 20 December 2004

where F_{0j} is the normalized amplitude of the j mode, and the differential equation matrix elements are defined as:

$$Q_{0j} = -j\sigma(z)s_0\zeta_{0j,0j}$$
$$V_{0j,0k} = -j\sigma(z)\frac{s_1}{2}\zeta_{0j,0k}\exp\left[-jz\left(\beta_{0j}-\beta_{0k}\pm\frac{2\pi}{\Lambda}\right)\right] \quad (15)$$

where $\sigma(z)$ is the slowly varying envelope of the grating, s_0 and s_1 are the coefficients of the first two Fourier components of the grating function S(z), β_{0j} is the propagation constant of the j mode, and Λ is the period of the grating.

The $\pm$ sign in the exponential function depends on the sign of the difference between the propagation constants of the modes, which permits the coupling between each pair of them. If $\beta_{0j} > \beta_{0k}$, the minus sign is selected; otherwise the plus sign is chosen.

The transmission can be found by assuming that only one mode is incident ($F_{01}(0)=1$ and $F_{02}(0)=\cdots\cdots=F_{0N}(0)=0$) and solving the differential equation. The transmission power at the end of the LPFG can be expressed as:

$$\frac{|F_{01}(L)|^2}{|F_{01}(0)|^2} \quad (16)$$

where L is the length of the grating.

If only the self coupling coefficients and the cross coupling coefficients between the core mode and the cladding modes are considered, the computational effort is one order of magnitude lower, but additional errors can be caused for gratings with strong refractive index modulation [14]. For this reason, the full matrix formulation is used.

Finally, important reduction in computational effort can be obtained if adequate selection of modes included in the coupled mode equations is done. A rule suggested [14] is to select those modes that satisfy the Bragg condition to within a:

$$\left|\beta_{01}(\lambda)-\beta_{0j}(\lambda)-\frac{2\pi}{\Lambda}\right| \le 10^{-3}\,\mu m^{-1} \quad (17)$$

However, it has been proved that in some cases important modes are discarded, which may lead to important errors. Consequently, this rule must be widened depending on the structure analysed. Other modes that can be discarded are those whose coupling coefficient $\zeta_{0j,0k}$ with the core mode is lower than $10^{-7}\mu m^{-1}$. Their contribution is negligible for the transmission spectrum.

2.4. Methods for calculation of resonance displacement

In the analysis of Section 3, one of the main purposes is to see the displacement of the resonance wavelengths as well as the parameter to measure (i.e., ambient refractive index), experiments a variation. For this reason, alternative solutions to the application of coupled mode equations can be used if it is only necessary to analyse the displacement of the resonance wavelength. In this way computational effort is reduced.

The first one is the calculation of the resonance wavelength with the Bragg condition:

$$\beta_{01}(\lambda)-\beta_{0j}(\lambda)=\frac{2\pi}{\Lambda} \quad (18)$$

where β_{01} and β_{0j} are the propagation constants of the core and the *j* cladding modes respectively, and Λ is the period of the grating. Results obtained present appreciable variations related to those values calculated with transmission curves. However, if the modified first-order Bragg condition is applied, errors are lower than 0.1% [14]:

$$\beta_{01}(\lambda)+s_0\zeta_{01,01}(\lambda)-\left(\beta_{0j}(\lambda)+s_0\zeta_{0j,0j}(\lambda)\right)=\frac{2\pi}{\Lambda} \quad (19)$$

#5675 - $15.00 US Received 8 November 2004; revised 20 December 2004; accepted 20 December 2004

If this error is compared with fabrication tolerances, it can be concluded that this approximation offers great advantages in terms of computational effort. Henceforward it will be used in some cases in next section. After seeing the better accuracy of this formulation compared to that of expression (18) we can conclude that self-coupling coefficients are more related to the modification of the resonance wavelength of the attenuation bands, whereas in expression (1) the cross-coupling coefficients modify the depth.

3. Analysis of LPFG structures with deposition of an overlay

A commercial LPFG is selected for the analysis performed in this section. A modulation of the core refractive index is induced in a SMF28 single mode fiber. The parameters of the LPFG are: core diameter of 8.3 um, cladding diameter 125 um, core refractive index 1.5362, cladding refractive index 1.5306, overlay refractive index 1.67 ([$PDDA^{+}$/PolyS-119^{-}]), period of the grating is 276 μm, and the length of the grating is 25 mm. The modulation is considered sinusoidal. Consequently $\sigma(z) = s_0 = s_1 = 1$. The amplitude of the modulation is 3×10^{-4}.

If an overlay of higher refractive index than the cladding is deposited on this LPFG, as the thickness of the overlay increases, cladding modes shift their effective index to higher values. When the overlay is thick enough, one of the cladding modes is guided by the overlay. It is exactly the highest state of energy that jumps to the overlay, which means that the highest effective index mode (lowest order cladding mode) becomes guided. This causes a reorganization of the effective index of the rest of modes. Higher order cladding modes than the one that is guided by the overlay will shift their effective index value towards the effective index of the immediate lower order cladding mode. As more material is deposited, the effective index distribution before deposition is recovered. The effective index of the eight cladding mode will be now that of the seventh one, the effective index of the seventh cladding mode will be that of the sixth mode, and so forth. The same is true for the resonance wavelength values. The phenomenon repeats as more material is deposited. This means that if the thickness continues to be increased, more modes are guided by the overlay and new reorganizations of cladding modes takes place. In Fig. 2 the effective index of the core mode and the first ten cladding modes is represented as a function of the overlay thickness for a fixed wavelength of 1200 nm. LP_{02}, LP_{03}, LP_{04}, LP_{05}, become guided at 300, 1200, 2100 and 3000 nm.

Around the thickness value at which each of these modes is guided by the overlay, higher cladding modes shift their effective index value to cover the energy state left by their predecessors.

This phenomenon can be understood in terms of reorganization of modes. There exist allowed states for the effective indices of the modes. When the structure is perturbed by the deposition of an overlay, there exist not-allowed states that coincide with the transition to guidance of a cladding mode in the overlay. This is confirmed by the fact that fields of cladding modes present maxima or minima at the interface between the cladding and the overlay. In other words, the mode profile is mutating to the profile of the lower mode. In Fig. 3, the transverse field as a function of the radius is represented for the LP_{05} mode at a wavelength of 1200 nm. Three cases are considered: no overlay, overlay of 300 nm (transition to guidance of a mode at the overlay), and overlay of 750 nm. It can be appreciated the shift of the field profile towards that of the LP_{04} before deposition started.

The immediate consequence of the shift in effective index is that it leads to a displacement in all the attenuation bands. The attenuation band corresponding with the eighth mode shifts the wavelength to that of the seventh mode; the same is true for the seventh mode that shifts the wavelength to the attenuation band of the sixth mode, and so forth. Furthermore, there is an optimal deposition thickness where the central wavelength shift as a function of the ambient refractive index will be highest. This is the optimum overlay thickness (OOT). This value depends mainly on two variables: the refractive index of the overlay, and the ambient refractive index. Consequently, a good choice for a high sensitive device to the external refractive index is to stop the deposition when the effective index value of a mode is located between the effective index of the mode itself before deposition, and that of the next lower

#5675 - $15.00 US Received 8 November 2004; revised 20 December 2004; accepted 20 December 2004

cladding mode before deposition. This is an approximate solution. To calculate a more exact value, either the modified Bragg condition or the couple mode equations explained in section 2 will be used.

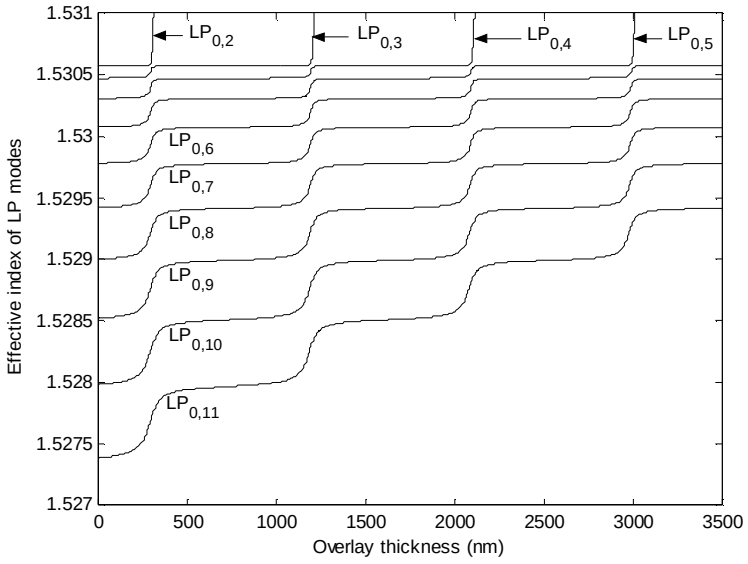

a)

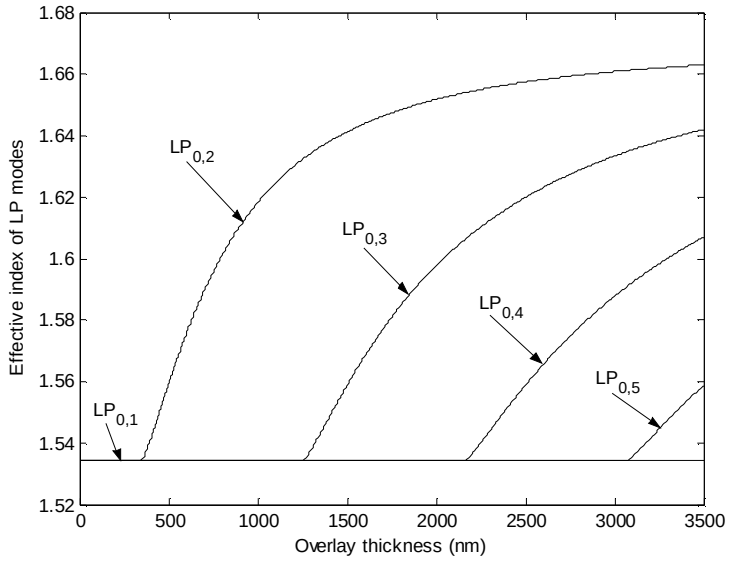

b)

Fig. 2. Effective index as a function of the overlay thickness of a) first ten cladding modes and b) core mode and first four cladding modes.

The modified Bragg condition is much more effective in terms of computation than the coupled mode equations. So, it is used for calculating the shift of the resonance wavelengths as a function of the overlay thickness. Three different refractive index materials are analysed in Fig. 4: 1.57 (tricosenic acid [24]), 1.62 ([PDDA^{+}/PolyR-47^{-}]), and 1.67 ([PDDA^{+}/PSS^{-}]).

#5675 - $15.00 US Received 8 November 2004; revised 20 December 2004; accepted 20 December 2004

As expected, the guiding starts faster if the overlay refractive index is higher. There are two important advantages in the usage of a higher refractive index overlay. The first one is that a lower amount of material is needed for the deposition. For adequate methods for nanodeposition, such as Electrostatic Self Assembly (ESA) [25], and Langmuir Blodgett (LB) this saves much time. Secondly, the transition to guidance of a cladding mode in the overlay is faster. This implies a higher variation of the effective index of the cladding modes as a function of the ambient refractive index, and a higher shift in the attenuation bands. For these reasons, the analysis will be continued with an overlay refractive index 1.67. The highest variation of the resonance wavelength is obtained at 278.5 nm, which is different from the value calculated for the classical Bragg condition: 267.5. Furthermore, there is a slight shift of the OOT for each mode considered. For instance, the fourth presents an optimum at 284 nm. Obviously it is not possible to obtain an optimum for each mode at the same time. However, the fact that the shift is not very important is proved in the next examples. Even if the optimum overlay thickness is not exactly fixed for a cladding mode, there is a range of values that also permits high sensitivities as a function of the ambient refractive index.

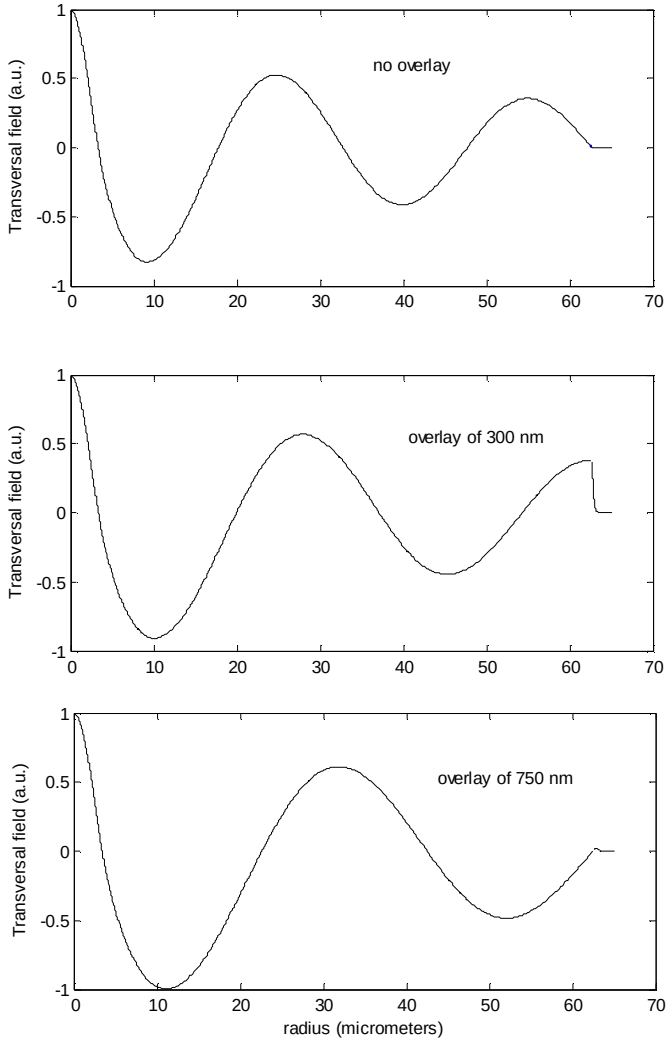

Fig. 3. Transverse electric field of the fifth cladding mode for three overlay thickness values: 0, 300, and 750 nm.

#5675 - $15.00 US Received 8 November 2004; revised 20 December 2004; accepted 20 December 2004

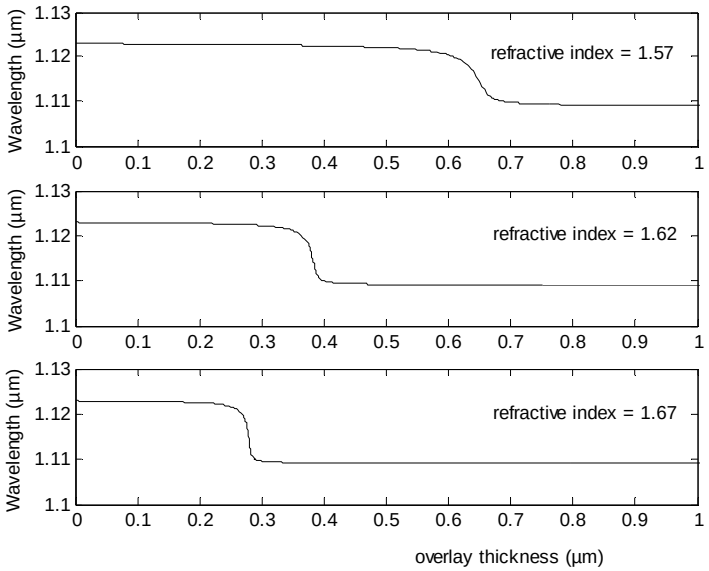

Fig. 4. Resonance wavelength shift in third cladding mode, as a function of the thickness of the overlay. Refractive indices of overlay: a) 1.57, b) 1.62 c) 1.67. Ambient index: 1.

Once the refractive index of the overlay is fixed, the versatility of this phenomenon is proved by the dependence of the OOT on a second parameter: the ambient refractive index. This permits to design refractometers sensitive to specific ranges of refractive indices. In Fig. 4 the design has been aimed for instance for gases. The OOT for the third mode is 278.5 nm for ambient refractive index 1. The purpose of using the OOT of the third cladding mode is to show that even for the case of lowest wavelength shift, the phenomenon is appreciable. In Fig. 5a, the change for three different ambient refractive indices in the transmission plot of an LPFG without overlay is compared. The shift in resonance wavelength is nearly unappreciable: 0.01, 0.03 and 0.05 nm respectively for the third fourth and fifth mode. On the other hand, if an overlay is added, in Fig. 5(b), dynamic ranges of 4.63 nm, 9.33 nm, and 8.34 nm for the third, fourth and fifth cladding mode resonance are obtained. These values are obtained even for a non optimum overlay thickness in the case of fourth and fifth resonance.

As a second example an important application is shown: the detection of oils. In this case, an optimum around an ambient refractive index 1.468 is selected. In Fig. 6 it is shown the evolution of the resonance wavelength caused by coupling between third, fourth and fifth cladding modes with the core mode. The decrease in the optimum thickness, as the ambient refractive index increases, is explained from slab waveguide theory. A slab between two different media starts guiding for a lower thickness as the refractive index of both media is more similar. When both media are the same it always guides. This theory can be extrapoled to cylindrical waveguides. There is a slight influence of the number of the mode in the optimum overlay thickness, and the range of displacement is higher for higher order modes. That is the reason for selecting in this case the optimum overlay thickness of the fifth mode: 159 nm. It is remarkable that the shape of the plot is very similar to the experimental results of [12] (Fig. 3 of such reference). In [12] the shift in fifth and sixth mode resonances of zone C is actually the sixth and seventh modes shift respectively, and the relative shift should be shifted to fit the values of zone A. Furthermore, in [19] it is proved theoretical results fit experimental ones.

#5675 - $15.00 US Received 8 November 2004; revised 20 December 2004; accepted 20 December 2004

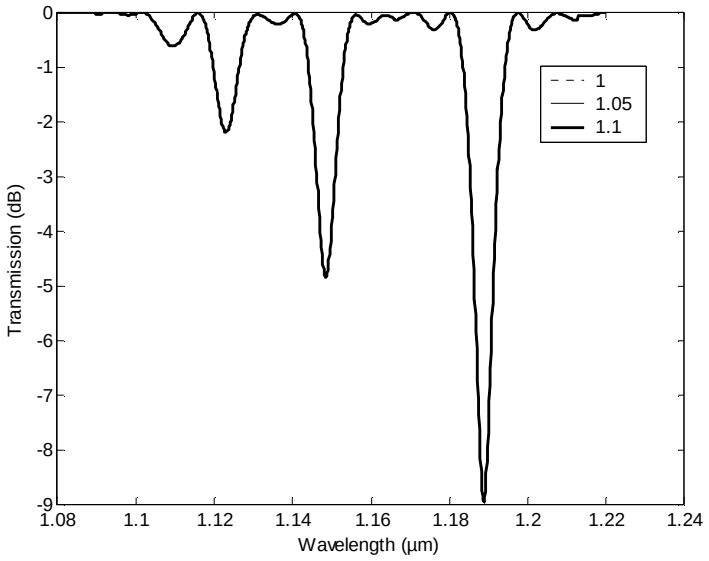

a)

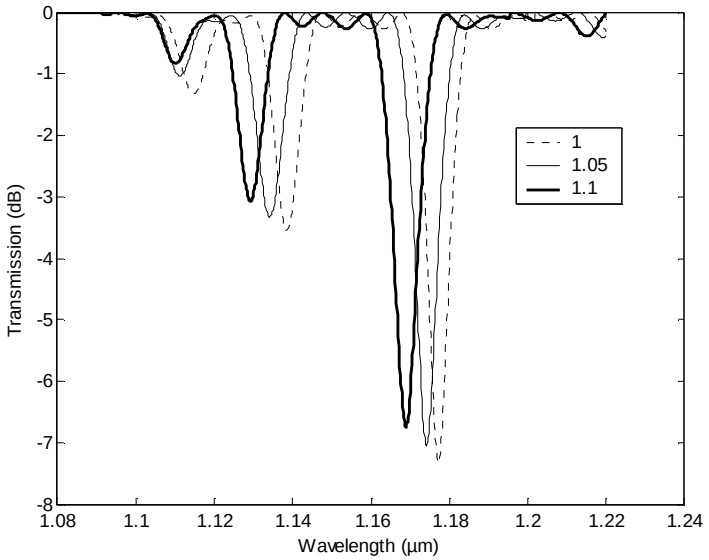

b)

Fig. 5. Transmission spectra of an LPFG as a function of three ambient refractive indices: 1, 1.05 and 1.1 a) without overlay b) with overlay of 278.5 nm and refractive index 1.67.

In Fig. 7(a) it is shown the shift in resonance wavelength of the fifth mode for an LPG where no overlay is added. Three different oils with refractive indices 1.461 (tee), 1.481 (cod) and 1.518 (tung) are analysed [26]. In Fig. 7(b), the same is done for an LPFG with overlay optimized for ambient refractive index 1.468. It can be clearly appreciated that the LPFG with overlay is also highly more sensitive than the other one in this case where the ambient refractive index is close to that of the cladding. There is an improvement in the sensitivity of the device of Fig. 7(a) in comparison with that of Fig. 5(a), but it is still far from the sensitivity obtained in Fig. 7(b). Between the first and the third refractive index there is a shift

#5675 - $15.00 US Received 8 November 2004; revised 20 December 2004; accepted 20 December 2004

for the fifth mode of 22.98 nm, whereas for the LPFG without overlay it is of 1.77 nm. A factor 12.98 of improvement has been obtained. Furthermore, a factor of 70.5 is obtained if we only consider tee and cod oils, because their refractive indices are closer to the refractive index the OOT has been calculated for.

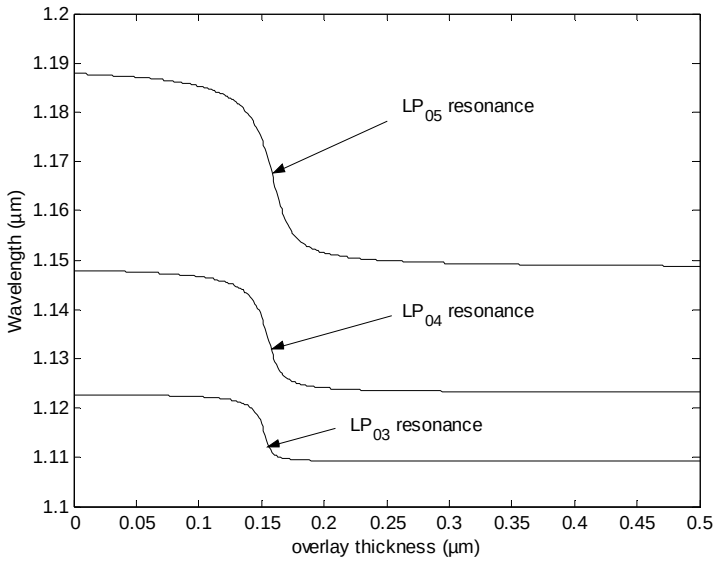

Fig. 6. Resonance wavelength shift in third, fourth and fifth cladding modes, as a function of the thickness of the overlay. Overlay refractive index: 1.67. Ambient index 1.468.

4. Conclusions

Calculation of the LP modes in a multilayer waveguide and coupled mode equations permits to obtain the transmission spectrum in an LPFG with an overlay. The approximation is valid for low order LP modes. This structure completes the other two cases studied so far for LPGs: ambient refractive index lower than the cladding [14, 16], and higher than the cladding [10, 17, 18]. Now a thin overlay is placed between the ambient and the cladding.

If the overlay presents a higher refractive index than the core, as its thickness is increased, it starts guiding the cladding modes with the highest effective index. In the transition of each of these modes to guidance in the overlay, there is a fast shift of the attenuation bands obtained in the transmission spectrum. This phenomenon has been analysed in terms of fields and allowed states of energy. Losses are not considered for the sake of simpler explanation of the phenomenon. In a next work the effect of losses in the overlay will be presented.

Many consequences are extracted from this. After selecting an overlay with an adequate refractive index, there is an optimum overlay thickness for each ambient refractive index. This optimum permits to obtain high sensitivity to low variations of the ambient refractive index itself. This avoids the limitation of LPFGs without cladding, where the highest sensitivity is obtained for those indices close to the cladding refractive index. Two examples have proved this fact. In the second one, even at optimum conditions for the LPG without overlay, the LPG with overlay offers a much better sensitivity. Other possible applications are the deposition of a material sensitive to a specific parameter. For instance a material whose refractive index is sensitive to oxygen will detect much lower concentrations if an overlay is deposited with an optimal thickness in air ambient conditions than typical LPFGs without deposition.

This technique will permit to extend even more the applications of LPFGs. Furthermore, the theory can be extrapoled to many sensor fields. So far dielectric structures studied are static. Here a dynamic structure has been analysed.

#5675 - $15.00 US Received 8 November 2004; revised 20 December 2004; accepted 20 December 2004

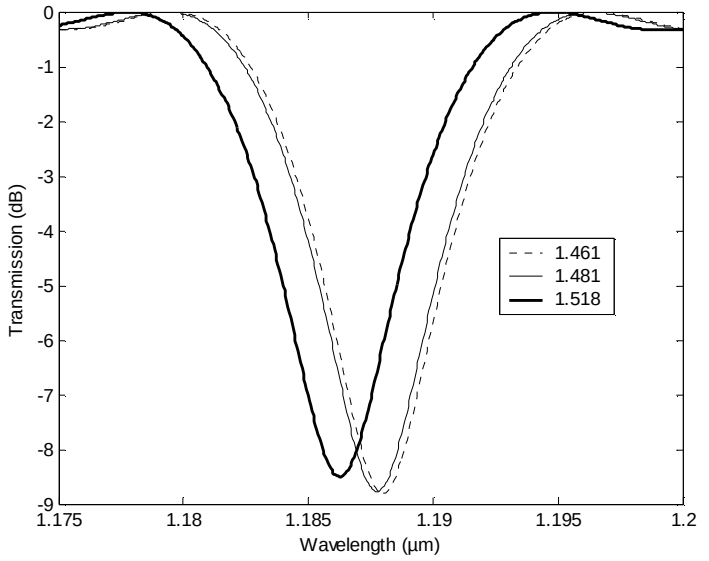

a)

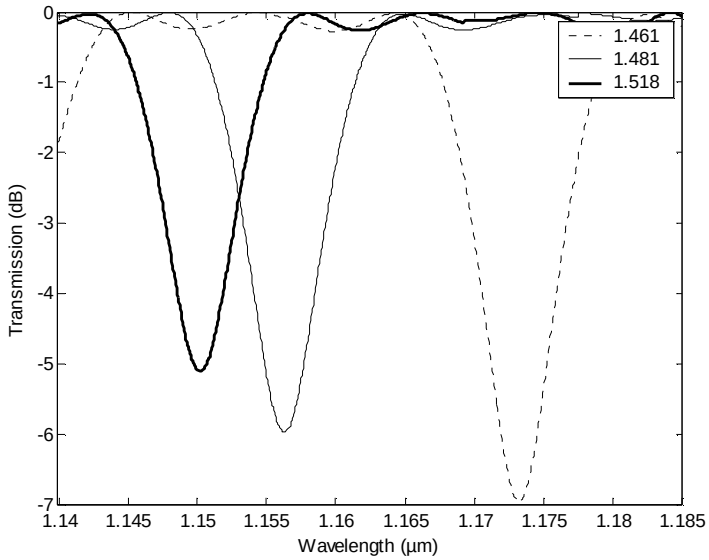

b)

Fig. 7. Transmittance spectra for the fifth cladding mode resonance of an LPFG for three oil refractive indices: 1.461, 1.481, 1.518. a) without overlay b) with overlay of 159 nm and refractive index 1.67.

Acknowledgments

This work was supported by Spanish Ministerio de Ciencia y Tecnologia and FEDER Research Grants CICYT-TIC 2003-00909, Gobierno de Navarra and FPU MECD Grant.

#5675 - $15.00 US Received 8 November 2004; revised 20 December 2004; accepted 20 December 2004